symmetry

MDPI

Article

Stability Analysis of Reverse-Dipping Rock Slopes Based on the Bi-Directional Evolutionary Structural Optimization Method (BESO) Prediction Method

Yu Zhang [1], Xuan Wang [1,2,*], Jiasheng Zhang [1,2], Honggang Wu [3] and Yingrun Chen [1]

[1] School of Civil Engineering, Central South University, Changsha 410075, China
[2] National Engineering Research Center of High-Speed Railway Construction Technology, Central South University, Changsha 410075, China
[3] Northwest Research Institute Co., Ltd. of CREC, Lanzhou 730070, China
* Correspondence: dddebug@csu.edu.cn

Abstract

Sliding failure is a common form of instability for reverse rock slopes. The determination of the failure plane for such unstable slopes is currently a key and challenging issue in research. To pinpoint the position of the failure surface with higher accuracy, this paper proposes a key equilibrium model based on the symmetric bidirectional evolutionary structural optimization (BESO) method. This model is based on the basic parameters of the slope, the BESO method, and the limit equilibrium theory. It uses its own algorithm program to search and determine the key failure plane of the slope. At the same time, two rock slope model tests were conducted to verify the effectiveness of this method in slope stability analysis. The calculated results exhibit a good consistency with the experimental outcomes, which confirms the feasibility of using the key equilibrium-bidirectional evolutionary structural optimization (CE-BESO) method for stability evaluation of this type of slopes.

Keywords: inclined rock slope; collapse damage; failure surface; critical equilibrium; two-way optimization

1. Introduction

Landslide failure is a typical instability mode for rock slopes [1]. Based on their dip directions, rock slopes can be categorized into anaclinal slopes and cataclinal slopes. Among them, the joint groups with steep inclination to the slope surface are the main characteristics of descending slope rock slopes [2,3]. Some scholars' statistical analysis of 100 rock slope failure cases in China indicates that 25% of the slope failures occur in slopes composed of intact blocky rock masses, 42% occur in ascending slopes, and 33% occur in descending slopes [4]. This shows that the proportion of descending slope rock slopes that experience failure among all failed rock slopes is much higher than what is commonly believed. A wealth of research on cataclinal slopes has been carried out by numerous scholars worldwide, and identifying the position of the failure surface remains a core and challenging issue in this field.

In practical engineering projects, bending-sliding failure is the predominant failure mode for cataclinal rock slopes when instability occurs, as illustrated in Figure 1 (a photograph of a slope subjected to bending-sliding failure). Besides the sliding failure of the rock layers within the slope body, the failure types of the anti-slip rock slope also include interlayer sliding failure of the rock layers and through-type failure that forms a continuous

Check for updates

Academic Editors: Quan Jiang and Chong Wang

Received: 10 December 2025
Revised: 19 January 2026
Accepted: 3 February 2026
Published: 13 February 2026

Copyright: © 2026 by the authors. Licensee MDPI, Basel, Switzerland. This article is an open access article distributed under the terms and conditions of the Creative Commons Attribution (CC BY) license.

failure surface [5–7]. Aydan and Kawamoto [8] successfully reproduced the bending and sliding of the slope using a bottom friction device and found that the entire failure surface is perpendicular to each layer of rock. Adhikary et al. [9] found based on the results of a set of centrifugal tests that the total failure surface of the slope extends from the foot of the slope to the top. The angle between the failure surface of the slope and the normal of the rock layer is approximately 12–20°. Moreover, some studies have found that the strength characteristics of joints and intact rocks have little influence on the range of the total failure surface angle [9–11]. The factors influencing the failure angle value are still unclear, but they may be related to the ratio of the slope height to the thickness of the rock layer [9]. Zheng [12] reproduced the bending and overturning phenomenon induced by the excavation of a rock slope on a highway in North China (Jingzhuoao Road) using two physical models. This study shows that the failure surface of the rock slope is multi-planar, not an ideal plane extending from the foot to the top.



(**a**) Bent and overturned deformation (**b**) Inverted body bending and cracking

Figure 1. A certain mountain body has undergone bending and collapse.

Numerical methods are also frequently employed to study the bending and collapse failure of inverted rock slopes. The advantage of these methods is that it is relatively easy to apply certain key physical quantities that are difficult to measure in model tests. For instance, using the two-dimensional discrete element method software (UDEC) can simulate the tensile or shear yield of intact rocks, as well as the sliding or opening of joints [13]. Moreover, it can simultaneously consider the failure of intact rocks and joints, making it a commonly used software for studying bending and collapse. Based on the strength reduction technique proposed by Dawson [14], Alessiano and Alonso [15] adopted UDEC and used it to calculate the safety factor for the bending and overturning of rock slopes. Subsequently, a large number of studies on bending and overturning were conducted at the laboratory or engineering scale. Li et al. [16] used UDEC to study the influence of geological layers on the formation of bending and overturning damage in large underground caverns, and found that bending and overturning were caused by multiple factors such as layer orientation, unfavorable structural planes, and excavation of underground caverns. Besides UDEC, there are many other numerical methods that can also be used to study the bending and overturning of rock masses, such as the relatively unique grid spring model, finite discrete element method, and numerical manifold method, etc. [17–26].

In addition to physical model tests and numerical methods, the limit equilibrium method is another common approach to study the bending-toppling failure of rock masses. Due to its simplicity and convenience, the limit equilibrium method is the most commonly used method in slope stability analysis [27–29]. Moreover, this method has been proven to be very useful in the analysis of bending and overturning [7,8,18,19]. Its first application in this aspect was proposed by Aydan and Kawamoto [8], who regarded each layer of rock as a cantilever beam under the combined action of gravity and the force acting on its side. They assumed that the entire failure surface was perpendicular to the joint and passed

through the toe of the slope. Subsequently, many scholars expanded the Aydan-Kawamoto method to study the bending and overturning failure in more complex situations, such as when there is a fracture surface that is not perpendicular to the joint [9], the failure caused by the combination of bending and shear of the rock layer [30], and considering the elastic deformation of the rock layer [31]. Zhang et al. [32] proposed a new LEM method for bending and overturning failure based on the evolution process by dividing the tensile stress area into the degraded tensile stress area and the advancing tensile stress area. Zhao et al. [33] divided the slope into the free deformation area and the compatible deformation area, and established a new bending and overturning failure analysis method that can be used to determine the safety factor of each rock layer.

In the field of slope stability analysis, scholars worldwide have carried out fruitful research. Via theoretical analysis, physical model tests, and numerical simulations, they have explored the instability and failure behaviors of slopes, providing a reliable reference basis for slope reinforcement engineering. However, shortcomings still exist in the stability analysis of cataclinal rock slopes. Unlike conventional sliding failure, cataclinal slopes exhibit a distinct failure mechanism and lack a single sliding base surface, leading to the imperfection of current stability evaluation methods. Furthermore, no mature theoretical approach has been established to determine the location and morphology of the unstable failure surface in such slopes—a crucial prerequisite for accurate slope stability assessment and engineering design. The primary objective of this study is to propose a method for predicting the failure surface and safety factor of rock slopes subjected to bending-sliding failure. Integrating the limit equilibrium method with the bidirectional evolutionary structural optimization (BESO) method, this approach enables the identification of critical failure surfaces with arbitrary shapes in rock slopes under bending-sliding action. Additionally, it facilitates convenient investigation into the impacts of slope structural parameters on the failure surface and safety factor. Overall, this method lays a solid foundation for the stability evaluation and engineering design of rock slopes prone to bending-sliding failure.

2. Introduction to the BESO Method

The Bidirectional Evolutionary Structural Optimization (BESO) method is a bidirectional progressive structural optimization technique. Topology optimization, in simple terms, refers to a mathematical computation method that integrates structural information. Its fundamental principle is to minimize the structural volume (or maximize structural stiffness) while satisfying specific constraint conditions. Specifically, topology optimization is a computational approach that achieves the optimal convergence result through structural mesh discretization—this convergence is deemed achieved when the variation in the objective function is less than the predefined convergence criterion.

The Principle of the BESO Method

The BESO method can increase the "efficient" elements that play a role in the subsequent iterations in the "high-performance" (such as high material stress) areas of the material. During the iterative process, it can add or delete elements to make the stress distribution of the structure uniform and increase its average stress level. Different from the SIMP method, BESO directly performs 0-1 interpolation without intermediate density values, and the optimization of the structural contour is more clearly visible. To explain the basic principle of BESO using the stiffness optimization mathematical model, its main purpose is to obtain the structure with the maximum stiffness while minimizing the flexibility. Taking the flexibility as the objective function and the element density as the design

variable, the optimal topology problem under the volume constraint can be established as the following continuum topology optimization model:

$$\min: \quad C = F^T U = U^T K U$$

$$sub: \quad F = KU$$

$$\sum_{i=1}^{n} v_i x_i = V^*, \; x_i \in \{x_{\min}, 1\}$$

In the equation, F is the structural load matrix, U is the displacement matrix, C is the structural flexibility (strain energy), K is the overall stiffness matrix, V^* is the overall stiffness matrix, v_i is the unit volume, x_i is the unit design variable, (can take the values of $x_{\min}$ and 1, representing virtual units and real units, respectively), and to prevent the stiffness matrix from being singular, $x_{\min}$ a small positive number is taken.

(1) Unit sensitivity index

Firstly, the change in structural compliance caused by the removal of any element—the element strain energy is defined as "element sensitivity", and the sensitivity is intended to represent the change in the response of compliance to the change in element density. Therefore, the contribution value of structural compliance in topology optimization can be characterized by the sensitivity of the structural elements. The BESO method updates the design variables through the element sensitivity α_i, and the element sensitivity expressed in terms of structural strain energy can be described as:

$$\alpha_i = \frac{\partial C}{\partial x_i} (i = 0, 1, 2 \ldots, n)$$

If the calculation is based on an irregular grid, then "element sensitivity" should take into account the influence of the element volume and adopt the strain energy density:

$$\alpha_i = \frac{\partial C}{v_i \partial x_i} (i = 0, 1, 2 \ldots, n)$$

Furthermore, the "unit sensitivity" of the virtual unit is initially assumed to be zero. Then, its corrected sensitivity is obtained through filtering strategies and averaging strategies, and whether it should be transformed into a real unit is determined based on the magnitude of the sensitivity.

(2) Sensitivity Filtering

To account for the influence of uneven grid division, in the study, the volume strain energy of the elements was used as the sensitivity value. During the optimization process, as elements were continuously deleted, sometimes it would lead to discontinuity of element sensitivity at the element boundaries, thereby causing the structural optimization results to have substructures in the form of a checkerboard (checkerboard phenomenon). To eliminate the checkerboard effect and overcome the grid dependence, a sensitivity filtering strategy was considered:

$$\alpha_x = \frac{\sum_i w(r_i)\alpha_i}{\sum_i w(r_i)} = \sum_i \left(\frac{w(r_i)\alpha_i}{\sum_i w(r_i)} \right) = \sum_i \eta_i \alpha_i$$

$$w(r_i) = \max(0, \; r_{\min} - r_i)(i = 0, 1, 2 \ldots, n)$$

In the formula, α_x represents the modified sensitivity of the target unit, r_i is the center distance between unit x and unit i, w is the sensitivity weight, $r_{\min}$ is the filtering radius, η_i is a weight factor independent of the sensitivity value.

This filtering strategy mainly replaces the indicators of individual units with weighted values of small-scale unit groups, as shown in Figure 2 which is the schematic diagram of the relationship solution. Taking the target unit x as the center, a search radius R is set. Within the circular coverage area, if it is a 3D graphic, it is the spherical range. The corrected sensitivity α_x of the target unit is obtained by averaging the sensitivity of each node according to the distance weight factor $w(r_i)$. The sensitivity of the node α_i is obtained by weighted summation according to the sensitivity of the connected units of the node and the distance weight coefficient. The distance weight coefficient w_j and the node sensitivity α_i are, respectively:

$$w_j = \frac{1}{M}\left(1 - \frac{r_{ji}}{\sum_{j=1}^{M} \alpha_j^e}\right)$$

$$\alpha_i = \sum_{j=1}^{M} \alpha_j^e$$

In the formula, M represents the number of elements connected to node i.

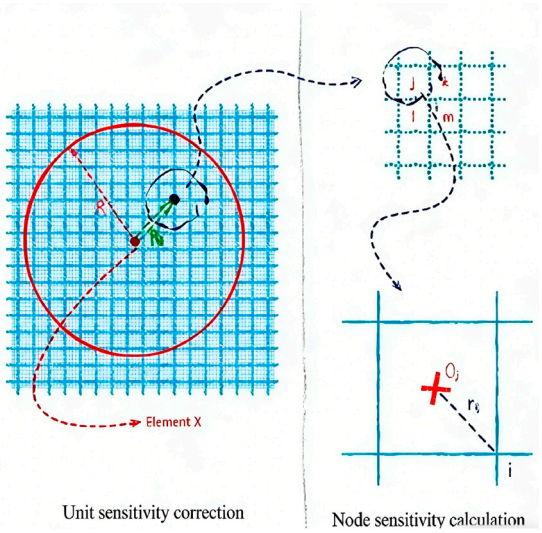


Figure 2. Graphical illustration of the relationship between element sensitivity correction and calculation in finite element computation.

The calculated sensitivity values are smoothed through unit sensitivity filtering, and the overall sensitivity of the design area units is optimized. Moreover, to ensure the stability of the iteration and prevent sudden changes in unit strain energy that lead to repeated increments and decrements, the unit sensitivity optimization process incorporates all the numerical information and performs historical iterative averaging on the sensitivity:

$$\alpha_k = \frac{\alpha_i^k + \alpha_i^{k-1}}{2}$$

In the formula, k represents the number of algorithm iterations during the search process.

(3) Unit addition and subtraction rules and unit convergence criteria

The BESO method controls the addition and deletion of elements by defining whether they meet the target volume V^*. If the structural volume V is greater than the target volume V^*, then deleting elements is the main approach; if the structural volume V is less than the target volume V^*, then adding elements is the main approach; if the structural volume V reaches the target volume V^*, then the remaining volume of the structure remains unchanged. The description of the structural volume in the optimization process can be expressed as:

$$V_{k+1} = V_k(1 \pm ER), (k = 1, 2, 3 \ldots)$$

As shown in Figure 3, it is a typical process of adding or reducing units. According to the filtering method, when performing a $k + 1$ unit addition or reduction operations, some virtual units will increase in sensitivity value after weighted correction, and their ranks will rise, entering the target volume. To avoid adding too many virtual units in a single step, an additional parameter, volume addition rate AR_{max}, is set to control the number of virtual units converted to real units in a single step. If the volume increase rate caused by the conversion of virtual units to real units meets the limit value, the unit deletion is performed according to V_{k+1}. If the volume increase rate exceeds the upper limit, the quantity of virtual units converted to real units is determined according to the limit value, and then the quantity of real units to be deleted is determined based on the sorting principle.

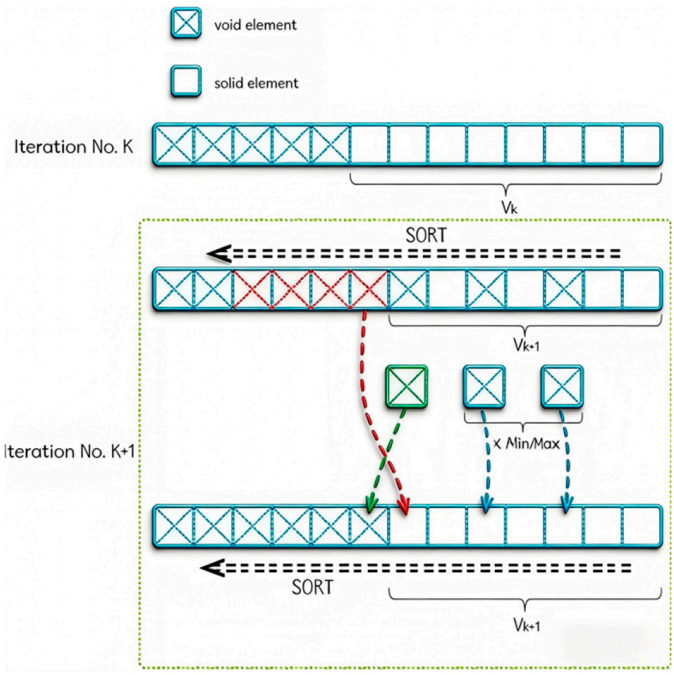


Figure 3. Schematic diagram of the typical unit elimination process in the BESO method.

In order to ensure the convergence of the objective function, the variation between iterations is set as the convergence criterion. When the total change in the objective function within multiple steps meets the requirements and the target volume is reached, the optimization process ends. From the above calculations, the sensitivity α_i of each node can be obtained. All elements in the structure are divided into two parts: high-sensitivity and low-sensitivity. Assuming that the threshold for deleting and adding element sensitivities are α_s and α_z, respectively, the following criteria are used to add and delete elements:

when $\alpha_i \leq \alpha_s$, the real units will be deleted;
when $\alpha_i > \alpha_z$, empty cells will be added.

The sensitivity is updated iteratively through the addition and deletion of units until the following convergence criterion is met:

$$error = \frac{\left|\sum_{i=1}^{N}(C_{k-i+1} - C_{k-N-i+1})\right|}{\sum_{i=1}^{N} C_{k-i+1}} \leq \tau$$

In the formula, N represents the parameter for the number of analysis steps selected.

3. Establishment of the CE-BESO Model

3.1. Model Establishment Concept

The model establishment idea is shown in Figure 4. Based on the basic principle and core idea of the bidirectional progressive structural optimization method (BESO) as described in the previous text, this paper uses the bidirectional progressive structural optimization method (BESO) to solve the failure surfaces of the reverse-sloping rock slope. In practical engineering, the reverse-sloping rock slope has complex structural planes and various surface joints. Therefore, this paper considers classifying the actual slope as a reverse-sloping rock slope discretized by joints, as shown in Figure 5, into slender rock layer strips.

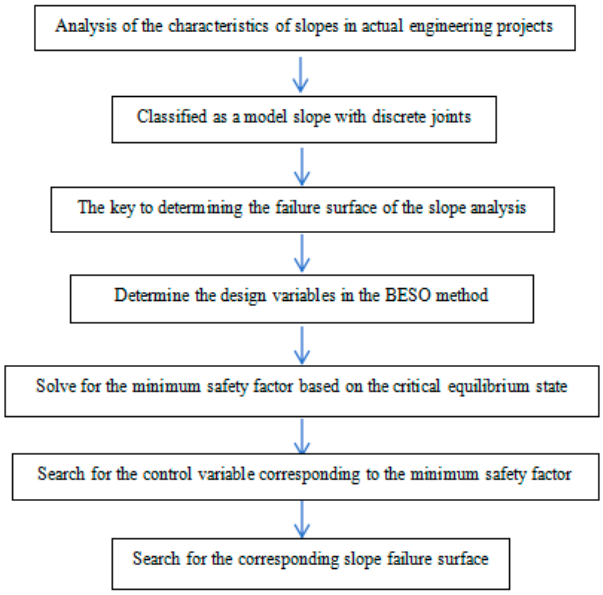


Figure 4. Conceptual diagram of model establishment.

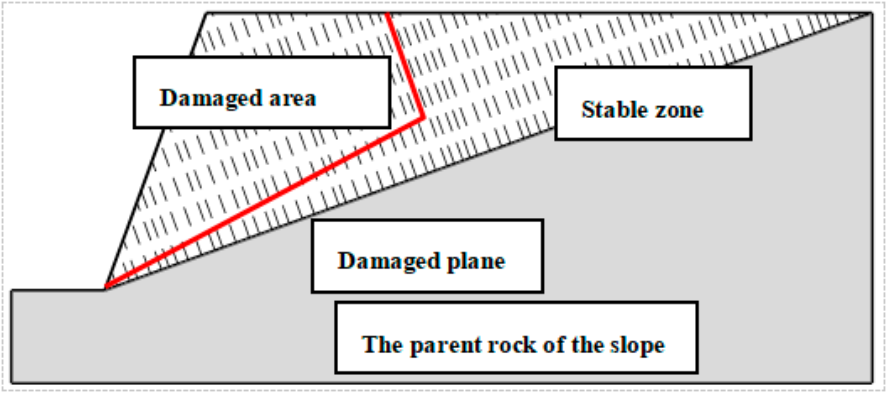


Figure 5. Schematic Diagram of Slope Model.

The failure surface of the slope can mainly be described by the distance between the potential failure surface of the slope and the slope surface. The slope surface is generalized as a plane perpendicular to the joint. To determine the predicted potential failure surface of the slope, this distance can be represented by a design variable. In order to better determine the classification principles of the parent rock of the slope, this paper divides the slope based on the relevant research results in references [34,35]. This variable can serve as a control variable for the discrete height of rock layers and also as a search variable in the BESO method. Therefore, by searching for the discrete height control variable corresponding to the minimum safety factor Fs, the potential failure surface of the studied slope can be obtained.

3.2. Strategy Diagram for Determining Slope Failure Surface

In this study, joints naturally divide the inverted rock slope into elongated rock layers. Therefore, the failure surface of the slope can be represented by the design variable $y = [y_1, y_2, \ldots, y_n]$, whose components, respectively, represent the heights of the discrete rock layers, and n is the number of discrete rock layers. $y_i = z_i / z_{ti}$, where it represents the distance between the predicted failure plane in the i-th soil-rock layer and the slope surface (the plane perpendicular to the joint). z_{ti} is the total height of the i-th soil-rock layer (the distance between the bedrock plane and the slope surface). Therefore, the potential failure plane of the studied slope can be searched by searching for the variable y_i corresponding to the minimum safety factor F_s. The variable y is a search variable in the BESO method.

3.3. Objective Function

In one iteration, the BESO method ultimately needs to determine a set of assumed failure planes rather than a single failure plane's corresponding safety factor. Therefore, the algorithm needs to be parallelized to reduce the required computing time. In this study, a target function was selected, whose purpose is to minimize the safety factor F_s. This target function can be expressed as:

$$\min : F_s = f(y, w, c, \phi)$$

$$sub : 0 < y_i < 1;\ z_{i-1} < z_i$$

Here, F_s represents the safety factor and w represents the weight of the rock.

3.4. Sensitivity Analysis

3.4.1. Definition of Sensitivity

The flowchart of the BESO algorithm is shown in Figure 6. To execute this optimization program, the BESO method needs to evaluate the sensitivity S_i of each variable y_i. The sensitivity S_i is defined as the differential of the safety factor with respect to variable y_i.

$$S_i = \frac{f([x_1, x_2, \ldots, x_i + \Delta x, \ldots, x_n], w, c, \phi) - f([x_1, x_2, \ldots, x_i, \ldots, x_n], w, c, \phi)}{\Delta x}$$

Here, in this article, the value of Δx is set to 1×10^{-6}. In this study, the function of the safety factor F_s is an explicit expression, while the sensitivity S_i is an implicit expression. Therefore, in this study, the sensitivity S_i is solved using different methods.

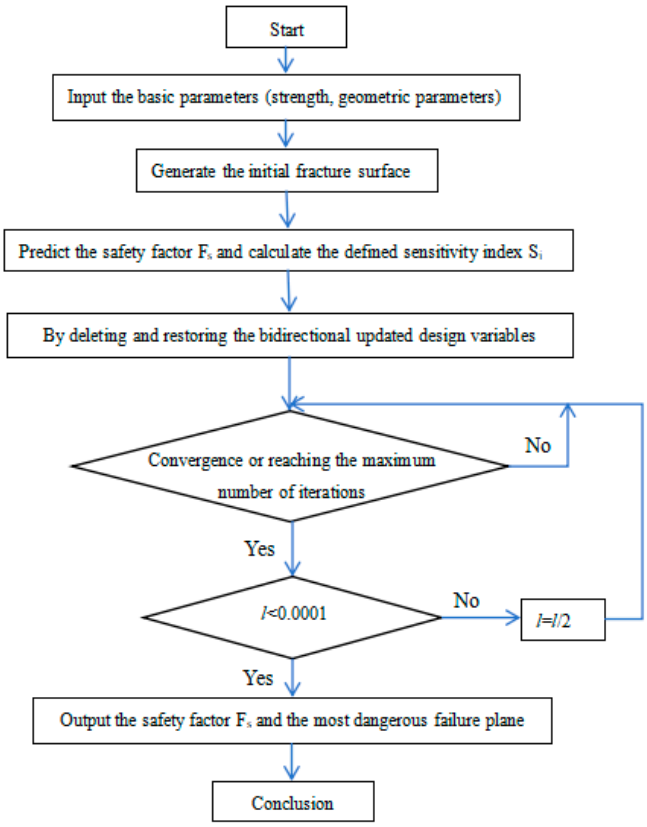


Figure 6. Flowchart of the CE-BESO Algorithm.

3.4.2. Sensitivity Calculation

In order to enhance the stability and convergence of this optimization program, this study calculated the sensitivity of each rock-soil layer unit and introduced the average change degree index $\overline{S_i}$, which is the average value of the sensitivity S_i obtained in the kth iteration and the sensitivity obtained in the $(k-1)$th iteration:

$$\overline{S_i} = \frac{S_i^{k-1} + S_i^k}{2}$$

Here, k represents the current iteration number. Then, the average value of the sensitivity calculated is assigned to the sensitivity of the current iteration and is used for the iteration of the next program $(k+1)$.

$$S_i^k = \overline{S_i}$$

In order to find the corresponding minimum safety factor F_s, in this study, the value of variable Z_i was updated by defining a control variable step size l.

$S_i > 0$, reduce the value of variable Z_i by controlling the step size l;

$S_i < 0$, increase the value of variable Z_i by controlling the step size l.

3.5. Analysis of the CE-BESO Model

3.5.1. Initial Value Setting

The BESO algorithm can calculate the corresponding safety factor F_s as Z_i changes and will form a new failure surface. The control variable step size l is set to 0.02 at the beginning of the algorithm. To improve the accuracy of the position of the critical failure surface of the slope obtained, after the feasible failure surface converges, the control variable step size l will be reduced to $l/2$. Then, the BESO program will repeatedly iterate until $l < 0.0001$ is

satisfied, and the corresponding critical failure surface with the minimum safety factor will be searched for.

3.5.2. Evaluation of the CE-BESO Model

Subsequently, MATLAB 2016a code was developed to implement the CE-BESO method. The code takes the geometric and mechanical parameters of the studied slope as input and outputs the safety factor and the potential failure plane of the slope. The final failure plane and safety factor are to some extent dependent on the randomly generated initial values. Different initial values will lead to differences in the final calculation results. This paper mainly selects the initial values based on the existing research [33]. The initial value θ is set as 12°, where θ is the angle between the defined initial failure plane and the plane perpendicular to the joint. Later, this angle is uniformly referred to as the initial angle. As shown in Figure 7, this is a schematic diagram of the initial failure plane position during the first iteration using the CE-BESO method.

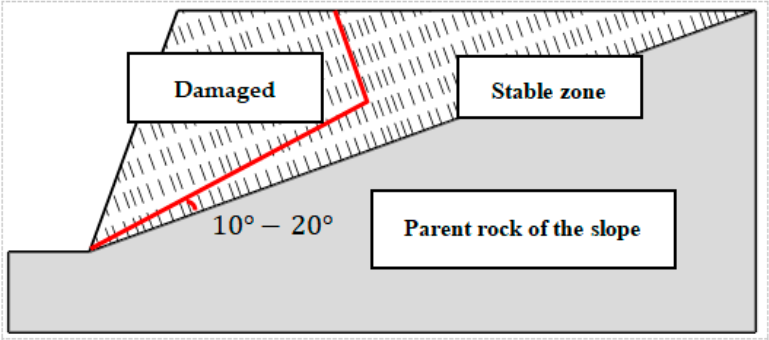


Figure 7. Schematic diagram of the initial failure plane position during the first iteration using the CE-BESO method.

4. Case Analysis of Backfilling Test for Rock Slopes Based on BESO Method

Based on the critical equilibrium state and its theoretical formula proposed in the previous section, as well as the topological principle of the bidirectional progressive structural optimization method (BESO), this section presents a theoretical model for studying the collapse failure of inverted rock slopes (CE-BESO). Two inverted rock slope test models from the literature [33,36] are taken as the research objects. The MATLAB 2016a stability analysis program is compiled to search for the failure surfaces of the slopes in the two tests, to verify the validity and applicability of the CE-BESO method proposed in this paper. Finally, the calculation results of this method are compared and analyzed with those of Zheng et al. [10] using the genetic algorithm, aiming to verify the effectiveness and accuracy of this method.

4.1. Analysis of Test Case 1

4.1.1. Introduction to Test Case 1

The first verification case experiment adopted in this study mainly focused on Zheng [10] et al.'s research on the failure mechanism of the slope when excavation occurs at the slope foot. As shown in Figure 8a, it is a photo of the test slope after typical bending and overturning failure due to the excavation at the slope foot. The slope model is shown in Figure 8b, and the slope is mainly divided into thin rock layers and thick rock layers (whose thickness is twice that of the thin rock layers). The basic parameters of the slope are shown in Table 1.

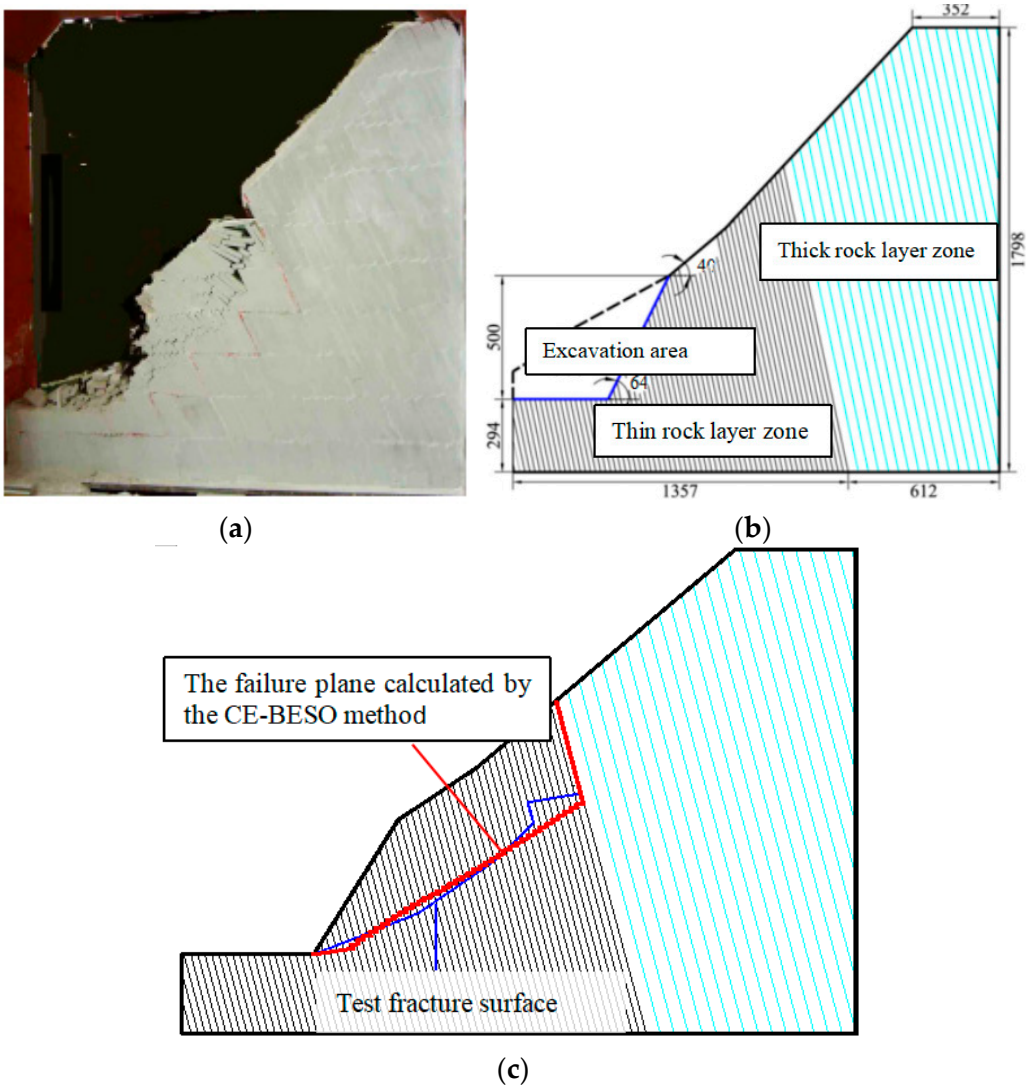


Figure 8. Verification analysis diagram of Case 1 (**a**) Slope undergoes bending and collapse failure (**b**) Model schematic diagram (unit: mm) (**c**) Comparison of test results and calculation results.

Table 1. Model parameters of test case 1.

Basic Parameters of the Slope Model	Parameter Value
Slope height Z (mm)	500
Slope angle α_s (°)	64
Rock cohesion c (Mpa)	0.028
Rock friction angle φ (°)	39
Rock weight w (kN/m^3)	1500
The tensile strength of rock mass σ_t (Mpa)	0.023
Thickness of rock layer strips l (mm)	20
Rock layer cohesion c_d (Mpa)	0
Friction angle of rock layer strips φ_d (°)	23
The angle between the direction of the rock layer's normal line and the vertical direction β_c (°)	12
Dimensionless parameters related to the normal stress μ	0.1
The angle (initial angle) between the initial plane and the bedding plane of the rock layer θ (°)	12 (10–20)

4.1.2. Calculation and Analysis of the CE-BESO Model 1

This paper uses the proposed BESO method to analyze the instability and failure of the model. This paper uses the proposed BESO method to analyze the instability and failure of the model. The calculation results are shown in Figure 8c. The failure plane determined by the BESO method is in good agreement with the results obtained from the experiment, and the calculation results are satisfactory. In addition, the safety factor calculated by the BESO method is 1.01, indicating that the model is essentially in the limit equilibrium state, which is consistent with the slope instability when the excavation reaches the corresponding depth in the experiment. The calculation results are in good agreement with the experimental results in the case, demonstrating the feasibility of using the CE-BESO method to predict the stability of reverse inclined rock slopes.

4.2. Analysis of Test Case 2

4.2.1. Introduction to Test Case 2

Adhikary et al. [9] conducted a series of centrifuge tests to study the mechanism of curved overturning failure. The second verification case adopted in this study mainly used the IGM model (mainly made of a mixture of ilmenite and gypsum (IGM) material). As shown in Figure 9a, the photo shows the failure of the IGM test slope when the gravitational acceleration reached approximately 80–85 g. The slope model is shown in Figure 9b, and the basic parameters of the slope are presented in Table 2.

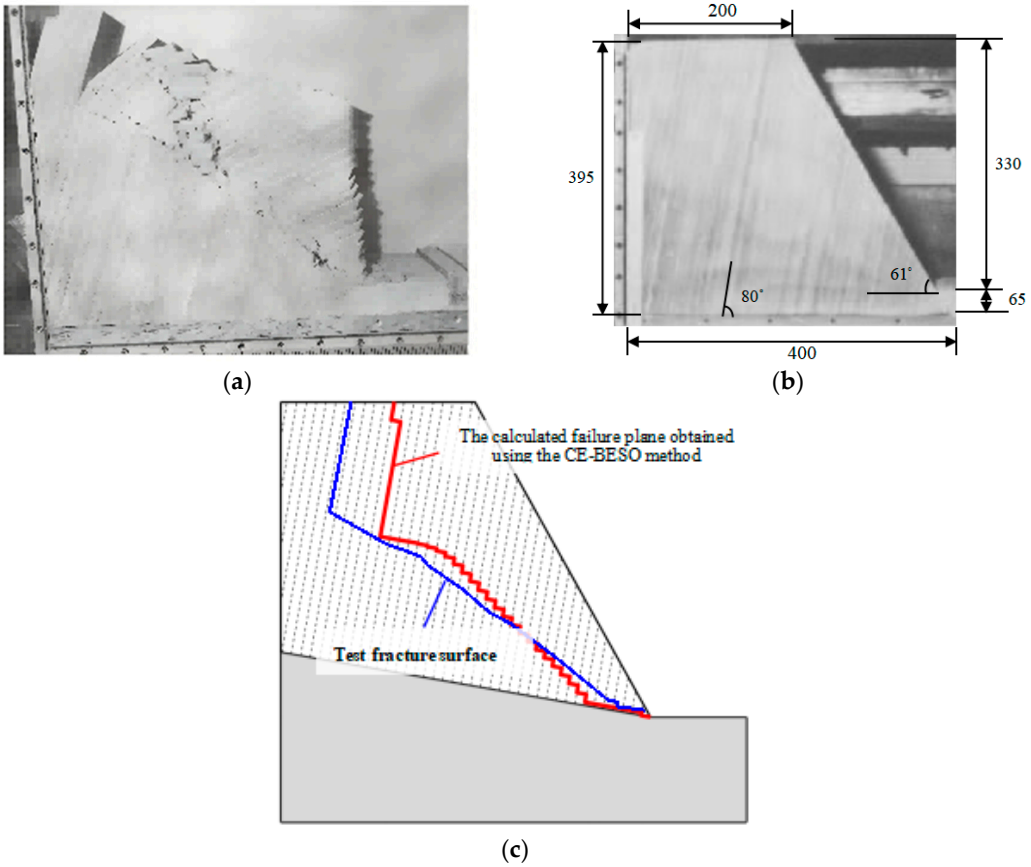


Figure 9. Verification analysis diagram for Case 2 (**a**) Slope undergoes bending and collapse failure (**b**) Model schematic diagram (unit: mm) (**c**) Comparison diagram of test results and calculation results.

Table 2. Model parameters of test case 2.

Basic Parameters of the Slope Model	Parameter Value
Slope height Z (mm)	330
Slope angle α_s (°)	61
Rock cohesion c (Mpa)	1.4
Rock friction angle φ (°)	37
Rock weight w (kN/m^3)	2380
The tensile strength of the rock mass σ_t (Mpa)	1.4
Thickness of rock layer strips l (mm)	10
Rock layer cohesion c_d (Mpa)	0
Friction angle of rock layer strips φ_d (°)	26
The angle between the direction of the rock layer's normal line and the vertical direction between the direction of the rock layer's normal line and the vertical direction β_c (°)	10
Dimensionless parameters related to the normal stress μ	0.1
The angle (initial angle) between the initial plane and the bedding plane of the rock layer θ (°)	12 (10–20)

4.2.2. Calculation and Analysis of the CE-BESO Model 2

As shown in Figure 9c, it is a comparison diagram of the results obtained by the BESO method search calculation and the actual test results of the failure surfaces. The results indicate that these two failure surfaces are basically consistent. This further confirms the effectiveness of the CE-BESO method proposed in this paper for the analysis of instability and failure of anti-tipping rock slopes.

5. Introduction to the CE-BESO Joint Analysis Model

The current research mainly focuses on anti-sagging rock slopes with relatively regular and uniform joint distributions. However, the situation of uneven joint distribution is rarely studied. In the existing literature that study the instability and failure mechanism of anti-sagging rock slopes, most of them are about anti-sagging rock slopes with uniform joint distributions [9,33]. However, in actual engineering, the common ones are rock slopes with uneven joint distributions. Zheng [10] et al. have used the LEM-GA method to study the influence of non-uniform joints on the stability of the slope. Therefore, this paper adopts the proposed CE-BESO method to study the influence of joint distribution on the stability of anti-sagging rock slopes. This paper mainly uses the test model in Case 2 for analysis. The relevant parameters needed for the calculation of this model are also shown in Table 2.

5.1. Numerical Calculation Results and Analysis of the Model

5.1.1. Analysis of the Impact of Uniform Distribution of Fissures

This paper employs the CE-BESO method to first generate an initial failure plane with an initial angle of 11°. It then analyzes the impact of uniform and random distribution of joints on the stability of the slope. In the uniform distribution case, the joint spacing is uniformly set at 10 mm, while for the random distribution, the spacing of each group of joints is randomly generated according to a function, and the total thickness of the joints is equal to that of the uniform distribution. Subsequently, using the CE-BESO method, the failure planes and safety factors corresponding to different g values under the uniform joint distribution are calculated, as well as the g value when the slope model fails under the random joint distribution. Due to the length of the article, this paper only selects the calculation results of four slope models with random joint distribution for analysis. The calculation results are shown in Figures 10 and 11, respectively.

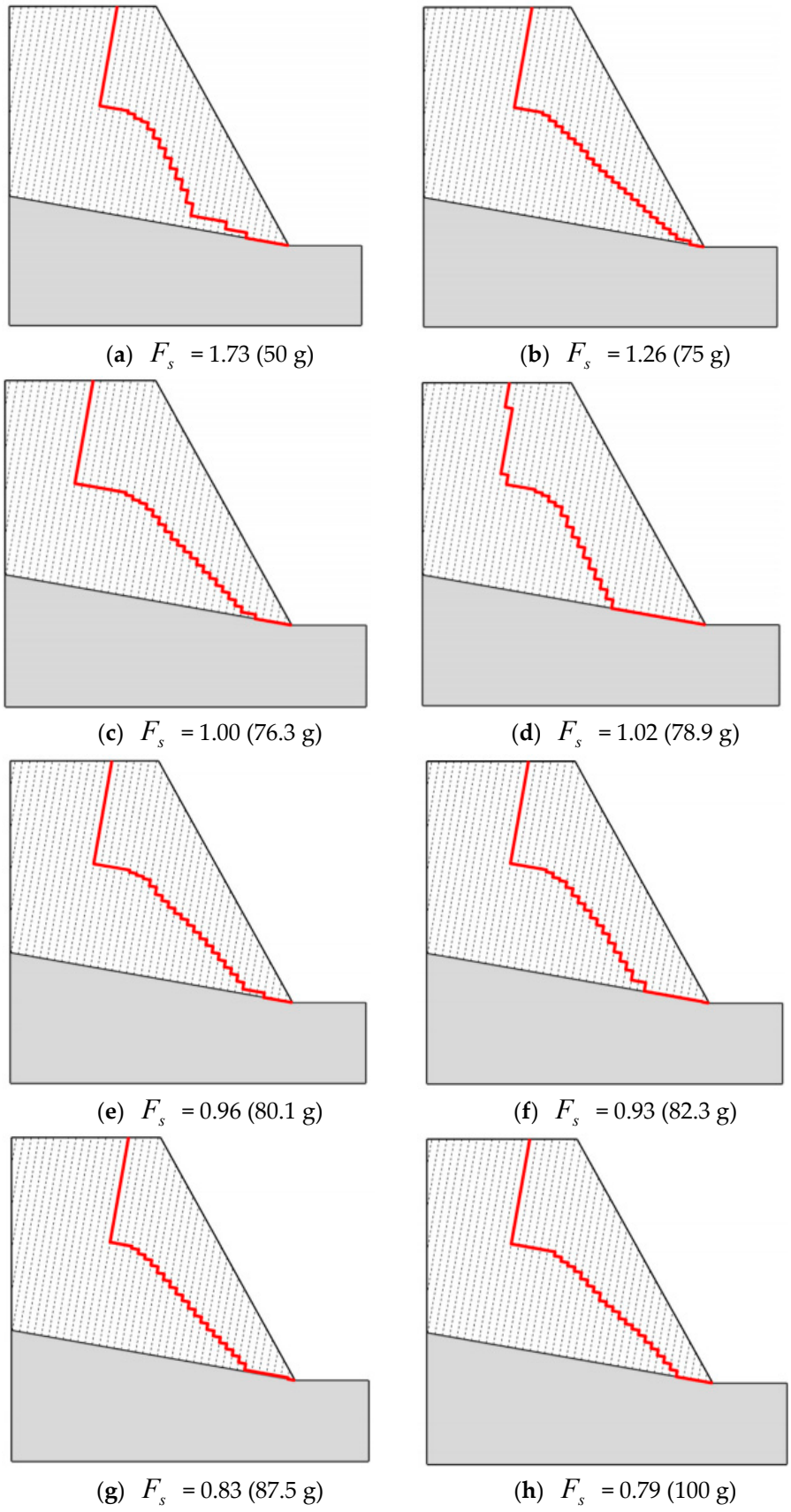


Figure 10. The critical failure plane calculated under different loading conditions (g), with the iteration stopping when the difference between the loading values is less than 0.1.

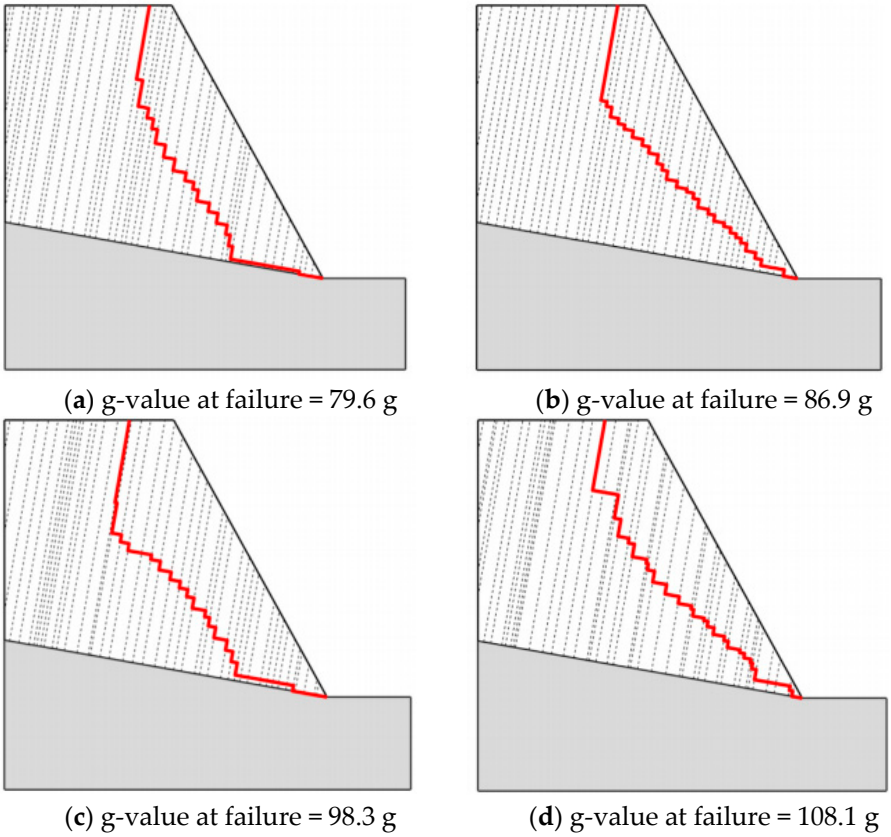


Figure 11. The corresponding load values (g) at which the four groups of slope models with random fracture distribution failed.

5.1.2. Comparative Analysis of Joint Distribution Situation

The calculation results of g values in the two cases were compared and analyzed as shown in Figure 12. Through the comparison and analysis, we can see that the g value at the time of instability and failure calculated for the model with random distribution of joints (79.6–108.1 g) is greater than that for the model with uniform distribution of joints (76.3 g). The obtained results are basically consistent with those obtained by Zheng [10] and others using the LEM-GA method. The g value calculated for the random distribution of joints is approximately 14.7% lower than that calculated for the uniform distribution of joints. Thus, we can see that the results obtained from the slope stability analysis under the condition of uniform joint distribution are more conservative.

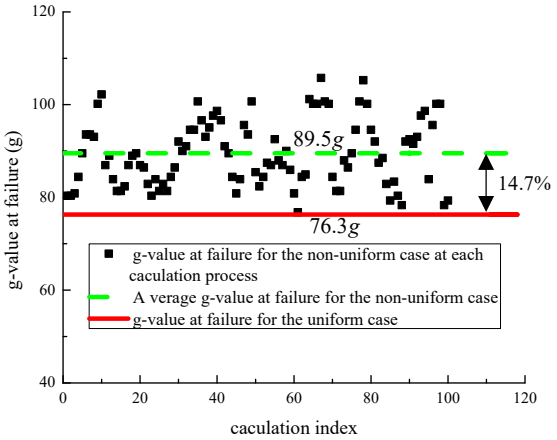


Figure 12. Comparison analysis diagram of loading g-values during failure under conditions of uniform and random distribution of fractures.

In the article by Zheng et al. [10] that studies the stability of reverse-dip rock slopes using the LEM-GA method, it is proposed that a three-layer cantilever beam can be used to explain why a conservative value is obtained when the joint distribution is uniform. Based on the cantilever beam theory, the bending resistance of a certain layer of rock stratum mainly depends on its moment of inertia $I_i = d_i^3/12$, as shown in Figure 13. The moment of inertia of the overall structure composed of these three layers of rock strata is:

$$I_e = \frac{d_i^3 + d_{ii}^3 + d_{iii}^3}{12}$$

In the formula, d_i, d_{ii}, d_{iii} represent the thicknesses of the rock layers in the *i*st, *ii*nd, and *iii*rd layers, respectively.

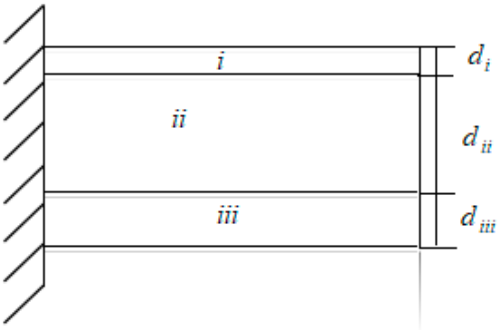


Figure 13. Schematic diagram of three-layered rock layers with different thicknesses, resembling cantilever beams.

From the formulas in this section, it can be seen that when the thickness of the three layers of rock strata is equal and constitutes one-third of their total thickness, the moment of inertia I_e of the overall structure formed by these three layers of rock strata reaches its minimum value. Thus, it can be concluded that when the joint distribution of the studied slope is uniform (with equal thickness of each rock layer), the corresponding moment of inertia is the smallest, so the force resisting failure is also the smallest, and the corresponding g value is more conservative when instability failure occurs.

5.2. The Distribution of Fractures Affects the Comprehensive Analysis

The random distribution of rock layer joints has a significant impact on the analysis results of slope stability. The four slope models are all the same except for the random distribution of joints. The total thickness of each rock layer and the number of rock layers are equal. As shown in Figure 14, the thickness distribution of the corresponding random rock layers for the four slopes is presented, with an average thickness of 10 mm. It can be clearly seen that when the slope fails, corresponding to different g values and failure planes, such as in Figure 11a where the failure occurs corresponding to g = 79.6 and in Figure 11d where the failure occurs corresponding to g = 108.1, there is a significant difference. This is because the stability of the inverted rock slope largely depends on the bending resistance of the rock layers near the toe of the slope [11]. When the moment of inertia value of the rock layers near the toe of the slope is larger, the slope is more stable. And as can be seen more intuitively from Figure 11, the thickness of the rock layer near the toe of the slope in Figure 11a is larger than that in Figure 11d, so the moment of inertia value of the former is larger than that of the latter. Therefore, the thickness of the rock layers near the toe of the slope has a significant impact on the stability of the slope.

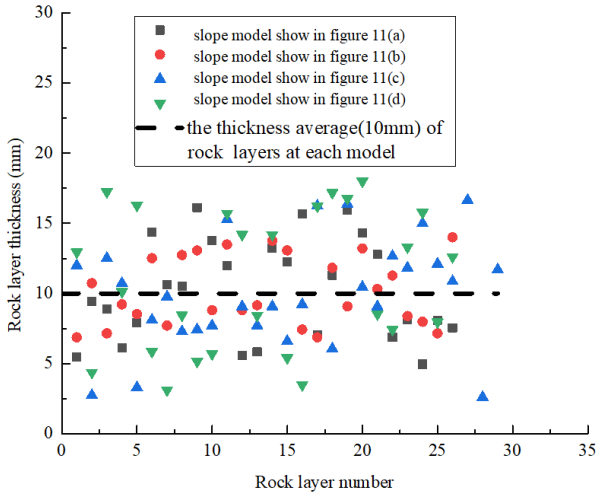


Figure 14. Scatter plot showing the distribution of rock layer thickness in the damaged area in Figure 11.

Based on the above analysis results, it is found that they are consistent with the analysis results in the article by Zheng [10] who used the LEM-GA method to study the stability of reverse inclined rock slopes. Moreover, this further verifies the effectiveness of the CE-BESO method proposed in this paper.

6. Conclusions

Based on the limit equilibrium theory, this study introduces the bidirectional evolutionary structural optimization (BESO) method to assess the stability of cataclinal rock slopes that have undergone collapse failure. A critical equilibrium (CE-BESO) model is proposed by integrating the BESO method. To implement the proposed critical equilibrium analysis approach, a MATLAB-based stability analysis program for cataclinal rock slopes is developed; meanwhile, two physical model tests of cataclinal rock slopes are conducted to verify the effectiveness of the proposed method. Finally, the research is extended to the application of the CE-BESO joint element analysis model, aiming to investigate the influence of the structural distribution characteristics of cataclinal rock slopes on their stability. Through the aforementioned research, the following conclusions are drawn in this paper:

(1) By introducing dimensionless variables distributed along the depth direction and the initial angle, a novel slope partitioning simulation strategy and an arbitrary failure surface simulation strategy were developed. A MATLAB-based BESO algorithm program was compiled to predict the slope safety factor and search for the slope's critical failure surface, thus verifying the feasibility of the proposed strategies.

(2) Through the comparative analysis of model test cases, the test results are in good agreement with the simulation results, which verifies that the CE-BESO method has good feasibility and applicability in the stability analysis of reverse-dip rock slopes.

(3) The distribution of jointing in the rock strata of reverse inclined rock slopes has a significant impact on the stability of the slope. The thicker the rock strata near the slope foot, the greater the moment of inertia of the rock strata at the slope foot, and the more stable the slope will be.

(4) Introducing the sensitivity split ratio can eliminate the influence of empirical calculations, and by conducting parameterized research, we can explore the weight values that approach the accurate results.

(5) Based on the tests of two physical models, this paper proposes a theoretical model applicable to rock slopes that may suffer from sliding, bending or flipping failure.

The validity and accuracy of the model have been verified. Finally, the possible angle differences among the base calculation plane, the sliding zone, the superimposed zone and the discontinuity surface are presented.

Author Contributions: Y.Z.: investigation, methodology, resources, data curation, formal analysis, validation, writing—original draft, revision and editing; X.W.: Conceptualization, writing—review, project administration, formal analysis; J.Z.: suggestions at the beginning, Review of manuscripts, logic analysis; H.W.: computer algorithm, suggestions at the beginning; Y.C.: supervision, writing—review. All authors have read and agreed to the published version of the manuscript.

Funding: This research was funded by Science and Technology Research and Development Plan of China Railway Co., Ltd., grant number 2022-Major Project-07 and Research of China Railway, grant number KF2025-077.

Data Availability Statement: The original contributions presented in this study are included in the article. Further inquiries can be directed to the corresponding author.

Acknowledgments: Thank you for the computing power support provided by the Supercomputing Center of Central South University; Thank you for the site provided by the School of Civil Engineering, Central South University; Thank you for the technical and manual support provided on site.

Conflicts of Interest: Author Honggang Wu was employed by the company Northwest Research Institute Co. Ltd. of CREC. The remaining authors declare that the research was conducted in the absence of any commercial or financial relationships that could be construed as a potential conflict of interest. The authors declare that this study received funding from Science and Technology Research and Development Plan of China Railway Co., Ltd. (2022-Major Project-07), grant number 2022-Major Project-07 and Research of China Railway, grant number KF2025-077. The funder was not involved in the study design, collection, analysis, interpretation of data, the writing of this article or the decision to submit it for publication.

References

1. Zheng, Y.; Chen, C.; Liu, T.; Liu, X.; Song, Y.; Zhou, Y. Analysis of Rock Slope Collapse Failure Under Slope Top Load. *Rock Soil Mech.* **2015**, *36*, 2639–2647+2658.
2. Liu, H.; Tang, L. *Dynamic Responses and Failure Mechanisms of Inclined and Inverted Rock Slopes Under Strong Vibrations*; Earthquake Press: Beijing, China, 2016.
3. Yang, Z.; Liu, S.; Liu, Y.; He, C.; Yang, W. Dynamic stability analysis of bedding-parallel and reverse-slip rock slopes under repeated microseismic actions. *Chin. J. Geotech. Eng.* **2018**, *40*, 1277–1286.
4. Huang, R.; Li, W. Formation, distribution and risk control of landslides in China. *J. Rock Mech. Geotech. Eng.* **2011**, *3*, 97–116. [CrossRef]
5. Wu, H.; Zhao, W.; Nian, T.; Song, H.; Zhang, Y. Centrifugal Model Test Study on Collapse Failure of Inverted Layered Rock Slope. *J. Hydraul. Eng.* **2018**, *49*, 223–231.
6. Li, C.; Xiao, Y.; Wang, Y.; Bu, L.; Hou, Z. Research Status and Trends of Deformation and Failure Mechanisms of Rock Slopes in High-altitude Cold Regions. *J. Eng. Sci.* **2019**, *41*, 1374–1386.
7. Liu, X.; Deng, Z.; Liu, Y.; Liu, S.; Lu, Y. Research on the cumulative damage and failure mode of horizontal layered rock slopes under seismic action. *Rock Soil Mech.* **2019**, *40*, 2507–2516.
8. Aydan, A.P.; Kawamoto, T. The stability of slopes and underground openings against flexural-toppling and their stabilisation. *Rock Mech. Rock Eng.* **1992**, *25*, 143–165. [CrossRef]
9. Adhikary, D.P.; Dyskin, A.V.; Jewell, R.J.; Stewart, D.P. A study of the mechanism of flexural toppling failure of rock slopes. *Rock Mech. Rock Eng.* **1997**, *30*, 75–93. [CrossRef]
10. Zheng, Y.; Chen, C.X.; Liu, T.T.; Zhang, H.N.; Xia, K.Z.; Liu, F. Study on the mechanisms of flexural toppling failure in anti-inclined rock slopes using numerical and limit equilibrium models. *Eng. Geol.* **2018**, *237*, 116–128. [CrossRef]
11. Alzo'ubi, A.K.; Martin, C.D.; Cruden, D.M. Influence of tensile strength on toppling failure in centrifuge tests. *Int. J. Rock Mech. Min. Sci.* **2010**, *47*, 974–982. [CrossRef]
12. Zheng, Y.; Chen, C.X.; Liu, T.T.; Xia, K.Z.; Liu, X.M. Stability analysis of rock slopes against sliding or flexural-toppling failure. *Bull. Eng. Geol. Environ.* **2018**, *77*, 1383–1403. [CrossRef]
13. Itasca. *UDEC, Version 4.0. User's Manual*; Itasca Consulting Group Inc.: Minneapolis, MN, USA, 2004.

14. Dawson, E.M.; Roth, W.H.; Drescher, A. Slope stability analysis by strength reduction. *Géotechnique* **1999**, *49*, 835–840. [CrossRef]
15. Alejano, L.R.; Alonso, E. Application of the 'shear and tensile strength reduction technique' to obtain factors of safety of toppling and footwall rock slopes. In Proceedings of the Impact of Human Activity on the Geological Environment—Proceedings of the International Symposium of the International Society for Rock Mechanics, Eurock, Brno, Czech Republic, 18–20 May 2005; pp. 7–13.
16. Li, A.; Dai, F.; Xu, N.W.; Gu, G.K.; Hu, Z.H. Analysis of a complex flexural toppling failure of large underground caverns in layered rock masses. *Rock Mech. Rock Eng.* **2019**, *52*, 3157–3158. [CrossRef]
17. Lian, J.J.; Li, Q.; Deng, X.F.; Zhao, G.F.; Chen, Z.Y. A numerical study on toppling failure of a jointed rock slope by using the distinct lattice spring model. *Rock Mech. Rock Eng.* **2018**, *51*, 513–530. [CrossRef]
18. Yan, C.Z.; Jiao, Y.Y.; Zheng, H. A fully coupled three-dimensional hydro-mechanical finite discrete element approach with real porous seepage for simulating 3D hydraulic fracturing. *Comput. Geotech.* **2018**, *96*, 73–89. [CrossRef]
19. Yan, C.; Jiao, Y.-Y. FDEM-TH3D: A three-dimensional coupled hydrothermal model for fractured rock. *Int. J. Numer. Anal. Methods Geomech.* **2019**, *43*, 415–440. [CrossRef]
20. Yan, C.Z.; Jiao, Y.Y. A 2D discrete heat transfer model considering the thermal resistance effect of fractures for simulating the thermal cracking of brittle materials. *Acta Geotech.* **2019**, *15*, 1303–1319. [CrossRef]
21. Zhang, G.; Zhao, Y.; Peng, X. Simulation of toppling failure of rock slope by numerical manifold method. *Int. J. Comput. Methods* **2010**, *7*, 167–189. [CrossRef]
22. Yang, Y.T.; Xu, D.D.; Zheng, H. Explicit discontinuous deformation analysis method with lumped mass matrix for highly discrete block system. *Int. J. Geomech.* **2018**, *18*, 04018098. [CrossRef]
23. Yang, Y.T.; Zheng, H. Direct approach to treatment of contact in numerical manifold method. *Int. J. Geomech.* **2017**, *17*, E4016012. [CrossRef]
24. Yang, Y.T.; Tang, X.H.; Zheng, H.; Liu, Q.S.; Liu, Z.J. Hydraulic fracturing modeling using the enriched numerical manifold method. *Appl. Math. Model.* **2018**, *53*, 462–486. [CrossRef]
25. Yang, Y.T.; Guo, H.W.; Fu, X.D.; Zheng, H. Boundary settings for the seismic dynamic response analysis of rock masses using the numerical manifold method. *Int. J. Numer. Anal. Methods Geomech.* **2018**, *42*, 1095–1122. [CrossRef]
26. Yang, Y.T.; Tang, X.H.; Zheng, H.; Liu, Q.S.; He, L. Three-dimensional fracture propagation with numerical manifold method. *Eng. Anal. Bound. Elem.* **2016**, *72*, 65–77. [CrossRef]
27. Eduardo, M.B.; Pierre, L.; Lemos, J.V. 3D stability analysis of gravity dams on sloped rock foundations using the limit equilibrium method. *Comput. Geotech.* **2012**, *44*, 147–156. [CrossRef]
28. Stianson, J.R.; Chan, D.; Fredlund, D.G. Role of admissibility criteria in limit equilibrium slope stability methods based on finite element stresses. *Comput. Geotech.* **2015**, *66*, 113–125. [CrossRef]
29. Liu, X.; Wang, Y.; Li, D.Q. Investigation of slope failure mode evolution during large deformation in spatially variable soils by random limit equilibrium and material point methods. *Comput. Geotech.* **2019**, *111*, 301–312. [CrossRef]
30. Zheng, Y.; Chen, C.X.; Liu, T.T.; Song, D.R.; Meng, F. Stability analysis of anti-dip bedding rock slopes locally reinforced by rock bolts. *Eng. Geo.* **2019**, *251*, 228–240. [CrossRef]
31. Amini, M.; Majdi, A.; Aydan, Ö. Stability analysis and the stabilisation of flexural toppling failure. *Rock Mech. Rock Eng.* **2009**, *42*, 751–782. [CrossRef]
32. Zhang, G.C.; Wang, F.; Zhang, H.; Tang, H.M.; Li, X.H.; Zhong, Y. New stability calculation method for rock slopes subject to flexural toppling failure. *Int. J. Rock Mech. Min. Sci.* **2018**, *106*, 319–328. [CrossRef]
33. Zhao, W.; Wang, R.Q.; Nian, T.K. Stability analysis of anti-dip rock slopes with flexural toppling failure based on deformation compatibility. *Rock Mech. Rock Eng.* **2020**, *53*, 3207–3221. [CrossRef]
34. Lin, H.; Zhang, W.; Guo, S.; Zhang, X.; Wang, L.; Zhang, J. Study on the Energy Evolution Mechanism and Fractal Characteristics of Coal Failure Under Dynamic Loading. *ACS Omega* **2025**, *10*, 54710–54719. [CrossRef] [PubMed]
35. Feng, D.; Zhenhua, L.; Songtao, L.; Xiaolei, L.; Guodong, L.; Xuan, F.; Hao, R.; Zhengzheng, C. Breaking Law of Overburden Rock and Key Mining Technology for Narrow Coal Pillar Working Face in Isolated Island. *Sci. Rep.* **2024**, *14*, 13045. [CrossRef] [PubMed]
36. Duan, R.; Bai, S. A Search Method for Critical Slip Surface of Rock Slope Based on Critical Slip Field. *Rock Soil Mech.* **2007**, *28*, 861–864+870.

Disclaimer/Publisher's Note: The statements, opinions and data contained in all publications are solely those of the individual author(s) and contributor(s) and not of MDPI and/or the editor(s). MDPI and/or the editor(s) disclaim responsibility for any injury to people or property resulting from any ideas, methods, instructions or products referred to in the content.